Comparison of the T-matrix and Helmholtz integral equation methods for wave scattering calculations

W. Tobocman
Physics Department, Case Western Reserve University, University Circle, Cleveland, Ohio 44106

(Received 25 May 1984; accepted for publication 13 September 1984)

Calculations of the scattering of acoustic waves by rigid prolate spheroids of various aspect ratios were performed with both the T-matrix method (TMM) and the Helmholtz integral equation method (HIEM) on the same computer to compare the numerical stability of the two methods. For spherical targets the TMM converged more rapidly than the HIEM, but with increasing aspect ratio the rate of convergence of the TMM deteriorated rapidly while that of the HIEM was only slightly reduced. Moreover, roundoff error quickly became a serious problem for the TMM with increasing aspect ratio while for the HIEM it posed no problem at all in the cases considered. The numerical difficulties of the TMM were exacerbated by the fact that the matrices which had to be inverted became increasingly more ill-conditioned as the number of partial waves was increased. For the HIEM, on the other hand, the matrices to be inverted became increasingly better-conditioned as their dimension increased with the order of the calculation.

PACS numbers: 43.20.Fn, 43.20.Bi

INTRODUCTION

The T-matrix method (TMM) has been widely used to calculate the scattering of acoustic, electromagnetic, and elastic waves from targets of irregular shape. The method was first developed by P. C. Waterman for electromagnetic waves.[1] It was subsequently extended to acoustic wave scattering,[2] the scattering of acoustic waves by elastic targets,[3] and to the scattering of elastic waves.[4] The Helmholtz integral equation method (HIEM), has principally been used for radiation calculations.[5] An early application to scattering was carried out by G. B. Bundrit,[6] who calculated acoustic wave scattering by rigid spheroids when the direction of incidence is parallel to the axis of symmetry. We have used the HIEM to calculate the scattering of acoustic waves by rigid spheroids[7] and by fluid spheroids[8] for arbitrary angles of incidence. Our results showed that the HIEM is a practical and efficient method for calculating wave scattering by irregularly shaped targets.

One might expect that because the HIEM does not employ an expansion of the wave field in a set of spherical or spheroidal waves, it would avoid some of the numerical problems that beset the TMM. Our purpose in this paper is to investigate that question. We report the results of calculations of the scattering of acoustic waves by rigid spheroids performed by both the TMM and the HIEM on the same computer, a Digital Equipment Corp. VAX 11/780. Our calculations revealed that

(1) The TMM converges more rapidly than the HIEM for spherical targets.

(2) The rate of convergence of the TMM deteriorates very rapidly with increasing aspect ratio while the rate of convergence of the HIEM shows very little change.

(3) The number of terms in the partial wave expansion used by the TMM was limited by the occurence of overflows or, equivalently, by devastating roundoff errors. This limitation became more onerous with increasing aspect ratio. No such difficulties were encountered with the HIEM as the integration mesh was refined.

(4) The numerical difficulties of the TMM are exacerbated by the fact that the matrix which must be inverted becomes rapidly more ill conditioned as one increases the number of partial waves. The opposite occurs for the HIEM; the matrix which is to be inverted becomes increasingly better conditioned as the integration mesh is refined.

In Sec. I we present the TMM and HIEM formalisms. The results of our calculations are described in Sec. II. We discuss our results in Sec. III.

I. THE TMM AND HIEM SCATTERING FORMALISMS

We consider a plane acoustic wave of wavenumber k propagating in a medium M and scattered by a rigid body B surrounded by the medium M. Let S be the interface between the scatterer B and the medium M. Then the Helmholtz integral formula[9] for the wave field ψ is

$$\psi^{(0)}(\mathbf{r}) + \oint_S dS'\, \psi(\mathbf{r}')\mathbf{n}' \cdot \nabla' G(\mathbf{r}, \mathbf{r}') = \psi(\mathbf{r}), \quad \mathbf{r} \in M, \tag{1a}$$

$$= \tfrac{1}{2}\psi(\mathbf{r}), \quad \mathbf{r} \in S, \tag{1b}$$

$$= 0, \quad \mathbf{r} \in B, \tag{1c}$$

where $\psi^{(0)}$ is the incident plane wave, $\mathbf{n}'$ is the unit outward normal to S at the point $\mathbf{r}'$, and G is the Green's function

$$G(\mathbf{r}, \mathbf{r}') = (4\pi|\mathbf{r} - \mathbf{r}'|)^{-1} \exp(ik\,|\mathbf{r} - \mathbf{r}'|). \tag{2}$$

The Helmholtz integral equation method (HIEM) utilizes Eq. (1b) as an integral equation for the wave field ψ on the interface S. The solution of this equation, the Helmholtz integral equation, is then substituted into the expression

$$T(\mathbf{k}) = -(4\pi)^{-1} \oint_S dS\, e^{-i\mathbf{k}\cdot\mathbf{r}} i\mathbf{n} \cdot \mathbf{k}\psi(\mathbf{r}) \tag{3}$$

for scattering amplitude. The scattering amplitude is defined by the requirement that far from the target B the scattered wave field assumes the purely outgoing asymptotic form

 0001-4966/85/020369-06$00.80

$$\psi_s(\mathbf{r}) = \psi(\mathbf{r}) - \psi^{(0)}(\mathbf{r}) \to T(\hat{kr}) r^{-1} \exp(ikr), \tag{4}$$

where r is the magnitude of $\mathbf{r}$ and $\hat{r} = \mathbf{r}/r$.

The T-matrix method (TMM), on the other hand, is based on Eq. (1a). Partial wave expansions for the incident wave

$$\psi^{(0)}(\mathbf{r}) = \exp(i\mathbf{k}_0 \cdot \mathbf{r}) = 4\pi \sum_{l,m} i^l Y_l^m(\hat{k}_0)^* Y_l^m(\hat{r}) j_l(kr), \tag{5}$$

where the $k_0 = k$, the scattered wave

$$\psi_s(\mathbf{r}) = \psi(\mathbf{r}) - \psi^{(0)}(\mathbf{r}) = 4\pi \sum_{l,m} i^l Y_l^m(\hat{r}) h_l^{(1)}(kr) t_{lm}, \tag{6}$$

and the Green's function

$$G(\mathbf{r},\mathbf{r}') = ik \sum_{l,m} Y_l^m(\hat{r}) Y_l^m(\hat{r}')^* h_l^{(1)}(kr_>) j_l(kr_<), \tag{7}$$

are introduced into Eq. (1a). Here Y_l^m is the spherical harmonic, j_l is the spherical Bessel function, and $h_l^{(1)}$ is the spherical Hankel function of the first kind. Then, provided that the point $\mathbf{r}$ is located outside a sphere concentric with the origin and enclosing the target B, Eq. (1a) becomes

$$\begin{aligned} \sum_{l,m} i^l Y_l^m(\hat{r}) h_l^{(1)}(kr) t_{lm} = \sum_{l,m} ik Y_l^m(\hat{r}) h_l^{(1)}(kr) \\ \times \oint_s dS' [\mathbf{n}' \cdot \nabla' Y_l^m(\hat{r}')^* j_l(kr')] \\ \times \sum_{l',m'} i^{l'} Y_{l'}^{m'}(\hat{r}') [Y_{l'}^{m'}(\hat{k}_0)^* j_{l'}(kr') \\ + (4\pi)^{-1} t_{lm} h_{l'}^{(1)}(kr')]. \end{aligned} \tag{8}$$

Since this equation holds for all values of $\mathbf{r}$ outside the sphere enclosing B and since the functions $Y_l^m(\hat{r})$ are orthogonal, Eq. (8) must hold term by term.

$$t_{lm} = \sum_{l',m'} [J_{lm,l'm'} Y_{l'}^{m'}(\hat{k}_0)^* + H_{lm,l'm'} t_{l'm'}], \tag{9a}$$

$$J_{lm,l'm'} = i^{l'-l+1} k \oint_s dS' Y_{l'}^{m'}(\hat{r}') \mathbf{n}' \cdot \nabla' Y_l^m(\hat{r}')^* j_l(kr'), \tag{9b}$$

$$H_{lm,l'm'} = i^{l'-l+1} k \oint_s dS' Y_{l'}^{m'}(\hat{r}') \mathbf{n}' \cdot \nabla' Y_l^m(\hat{r}')^* h_l^{(1)}(kr'). \tag{9c}$$

In matrix notation Eq. (9a) reads

$$t = JY^* + Ht. \tag{10}$$

Upon truncation of the sum on partial waves, Eq. (10) can be solved by matrix inversion.

$$t = (1 - H)^{-1}, \quad JY^* = \mathcal{T} Y^* \tag{11}$$

$\mathcal{T} = (1 - H)^{-1} J$ is the T-matrix. The result is then used to calculate the scattering amplitude by means of

$$T(\mathbf{k}) = \langle \phi(\mathbf{k}) | t \rangle = \sum_{l,m} \phi_{lm}^*(\mathbf{k}) t_{lm}, \tag{12a}$$

where

$$\phi_{lm}(\mathbf{k}) = 4\pi i k^{-1} Y_l^m(\hat{k})^*. \tag{12b}$$

As the number of terms included in the partial wave sum is increased and the dimension of the matrices J and H increase accordingly, we expect the solution of Eq. (11) to converge to the exact values.

Return now to the Helmholtz integral equation [Eq. (1b)]. To solve it we emply a discretization process to transform it into a matrix equation which is subsequently solved by matrix inversion. The discretization process consists in dividing the interface S into N patches of roughly equal area. Let the area of the αth patch be A_α and let $\mathbf{r}_\alpha$ be a point near its center. Eq. (1b) is then approximated by

$$0.5\psi_\alpha = \psi_\alpha^{(0)} + \sum_{\beta=1}^{N} K_{\alpha\beta} \psi_\beta, \tag{13a}$$

where

$$\psi_\alpha = \psi(\mathbf{r}_\alpha), \quad \psi_\alpha^{(0)} = \psi^{(0)}(\mathbf{r}_\alpha), \tag{13b}$$

and

$$K_{\alpha\beta} = \mathbf{n}_\beta \cdot \nabla_\beta G(\mathbf{r}_\alpha, \mathbf{r}_\beta) A_\beta, \quad \alpha \neq \beta, \tag{13c}$$

$$K_{\alpha\alpha} = \int_{A_\alpha} dS' \mathbf{n}' \cdot \nabla' G(\mathbf{r}_\alpha, r'). \tag{13d}$$

In Eq. (13d) the integration is confined to the αth patch. The integral is evaluated in closed form using the lowest order terms of Taylor's series expansions about $\mathbf{r}_\alpha$. Similarly, Eq. (3) is approximated by

$$T(\mathbf{k}) = -(4\pi)^{-1} \sum_{\alpha=1}^{N} A_\alpha e^{-i\mathbf{k}\cdot\mathbf{r}_\alpha} i\mathbf{n}_\alpha \cdot \mathbf{k} \psi_\alpha. \tag{14}$$

In matrix notation Eqs. (13) and (14) become

$$\psi = 2\psi^{(0)} + 2K\psi, \tag{15}$$

and

$$T(\mathbf{k}) = \langle \chi(\mathbf{k}) | \psi \rangle = \sum_{\alpha=1}^{N} \chi_\alpha(\mathbf{k})^* \psi_\alpha, \tag{16a}$$

where

$$\chi_\alpha(\mathbf{k}) = i\mathbf{n}_\alpha \cdot \mathbf{k} (4\pi)^{-1} A_\alpha \exp(i\mathbf{k} \cdot \mathbf{r}_\alpha). \tag{16b}$$

Equation (15) is solved by matrix inversion

$$\psi = (1 - 2K)^{-1} 2\psi^{(0)}, \tag{17}$$

and the solution is substituted into Eq. (16) to get the scattering amplitude. We expect that as N is increased and the dimension of the matrix K increases accordingly, the solution of Eq. (17) will converge to the exact values.

Thus Eqs. (11) and (12) constitute the T-matrix method (TMM) and Eqs. (16) and (17) constitute the Helmholtz integral equation method (HIEM). For the general case we expect that the HIEM calculation will be much faster than the TMM because the elements of the matrix K in Eq. (17) are given by simple algebraic expressions from Eqs. (13c) and (13d) while the elements of the matrices J and H which appear in Eq. (11) must be calculated by two-dimensional integrals from tables of spherical harmonics and spherical Bessel and Hankel functions as shown in Eqs. (9). However, for an axially symmetric target like our spheroids the TMM has the advantage over the HIEM in that the TMM can exploit the axial symmetry of the target. It does this by taking the z axis

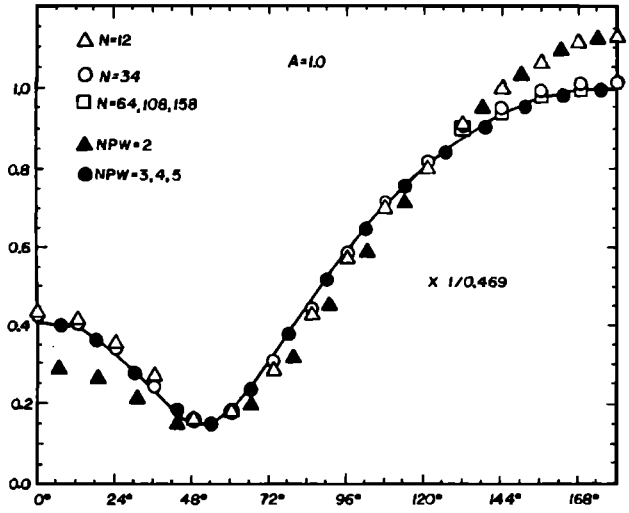

FIG. 1. Scattering amplitude $|T(\theta)|$ as a function of the scattering angle θ for a plane acoustic wave of wavenumber $k = 1.0$ incident on a rigid prolate spheroid of major semiaxis $c = 1.0$ and minor semiaxis $a = 1.0$. The direction of incidence is perpendicular to the axis of symmetry and the scattering plane is that of the symmetry axis and the direction of incidence. The open symbols represent values calculated with the HIEM using N patches. The solid symbols represent values calculated with the TMM using NPW partial waves. The curve is the exact result.

along the symmetry axis and finding in consequence that the matrices J and H are diagonal in m:

$$J_{l'm',lm} = \delta_{mm'} J_{l'm,lm}, \tag{18a}$$

$$H_{l'm',lm} = \delta_{mm'} H_{l'm,lm}. \tag{18b}$$

Thus in calculating the inverse of $1 - H$ in Eq. (11) we need only invert the submatrices associated with each value of m. In addition, the integrals shown in Eqs. (9) reduce to one-dimensional integrals simplifying their evaluation considerably.

II. CALCULATION OF THE SCATTERING BY RIGID SPHEROIDS

To compare the TMM and HIEM we apply them to the calculation of the scattering of acoustic waves by a rigid prolate spheriod. An example of the application of the T-matrix

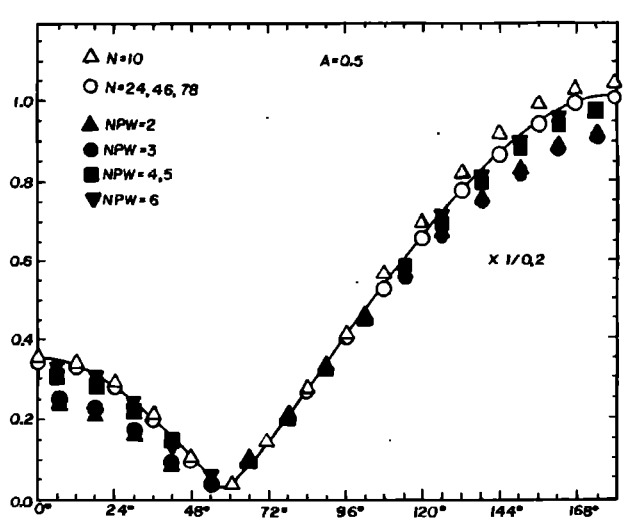

FIG. 2. Same as Fig. 1 except that $a = 0.5$ and the curve is merely drawn to aid the eye.

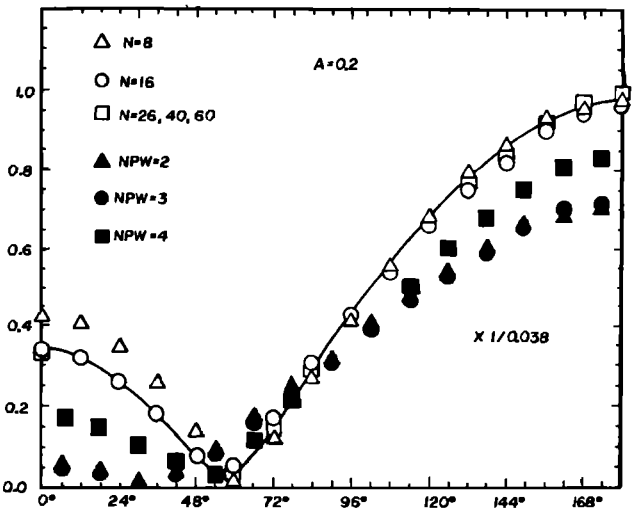

FIG. 3. Same as Fig. 2 except that $a = 0.2$.

method to this problem is found in the article by Varadan *et al.*,[10] which also contains references to earlier calculations using the separation of variables technique.

In Figs. 1–4, we display the results of calculating the scattering amplitude $|T(\mathbf{k})|$ for a plane acoustic wave of wavenumber $k = 1.0$ incident on a rigid prolate spheroid. The major semiaxis is $c = 1.0$ while the minor semiaxis is set equal to $a = 1.0$ in Fig. 1, $a = 0.5$ in Fig. 2, $a = 0.2$ in Fig. 3, and $a = 0.1$ in Fig. 4. The direction of incidence was taken to be perpendicular to the major axis of the spheroid. The scattering plane was taken to be the plane of the direction of incidence and the major axis.

In Fig. 1, the curve represents the exact scattering amplitude calculated by imposing the rigid body boundary condition in spherical coordinates. In the other three figures the curves have been drawn merely to aid the eye and are not the result of any calculation. However, the curves in Figs. 3 and 4 will be found to agree pretty well with scattering amplitudes calculated by Spence and Granger[11] using boundary condition matching in spheroidal coordinates.

The calculated points are identifed with respect to the

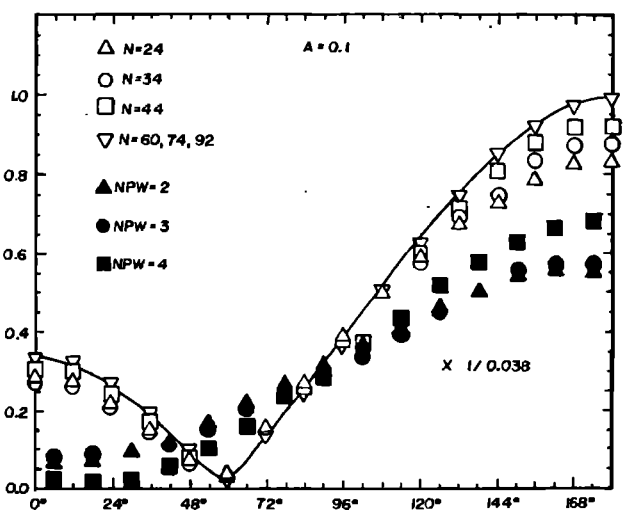

FIG. 4. Same as Fig. 2 except that $a = 0.1$.

TABLE I. Same as Fig. 1 except that $k = 6.0$. C. No. is the condition-number and NGP is the number of meshpoints used in the Gaussian quadrature procedure.

			$a = 1.0$ $k = 6.0$					
	HIEM					TMM		
N	C No.	$\lvert T(0°)\rvert$	$\lvert T(180°)\rvert$	NGP	NPW	C No.	$\lvert T(0°)\rvert$	$\lvert T(180°)\rvert$
12	5.97	1.202	1.269	48	5	1.01	1.796	0.6001
34	1.68	4.325	1.987	48	6	1.01	1.844	0.1084
64	1.46	2.545	0.8494	48	7	317	2.114	0.7595
108	1.28	2.344	0.3991	48	8	1.1×10^3	2.235	0.4769
158	1.19	2.316	0.5085	56	8	1.8×10^3	2.235	0.4769
				104	8	5.0×10^5	2.235	0.4769
	Exact	2.267	0.5309	48	9	6.0×10^7	2.262	0.5399
				48	10	overflow		
						Exact	2.267	0.5309

number of partial waves (NPW) employed in the case of the TMM and the number of surface patches (N) employed in the case of the HIEM. For the TMM calculation we found that our matrix inversion subroutine found $1 - H$ [Eq. (11)] to be singular for NPW > 7 when $a = 1.0$, for NPW > 6 when $a = 0.5$, and for NPW > 4 when $a = 0.2$ or 0.1. This is a consequence of the fact that the matrix elements $H_{lm,l'm'}$ defined in Eq. (9c) become greater in magnitude as l is increased due to the presence of the irregular Bessel function $h_l^{(1)}$ in the integrand. This effect becomes more serious with increasing aspect ratio c/a. When the matrix elements in the higher l rows get to be too large, the elements in those of lower l are effectively zero due to roundoff. The matrix is then singular to all intents and purposes.

Sometimes instead of finding $1 - H$ singular when NPW was too large the program would come to a halt because of an overflow. Of course, these difficulties could be alleviated to a certain degree by doing the calculation with double precision arithmetic or using a computer with a larger word size. For the HIEM calculation we encountered no such numerical problems in increasing N to 158, which was adequate for the cases considered here.

From Fig. 1, we see that for the spherical case the TMM calculation has converged at NPW = 3, so a breakdown at NPW = 8 is of no consequence. From Fig. 2, we see that for the aspect ratio = 2 case the breakdown of the TMM calculation at NPW = 7 means that it has failed by a small amount to converge to the correct value. In Figs. 3 and 4, we see that the breakdown of the TMM results in increasingly more serious error as the aspect ratio is increased.

We have repeated the series of calculations just described for $k = 6.0$ in place of $k = 1.0$. The deterioration of the convergence of the TMM calculation with increasing aspect ratio turns out to be even more serious for $k = 6.0$ than it is for $k = 1.0$. The immunity to increases of c/a of the convergence rate of the HIEM, on the other hand, remains intact. We have chosen to present the $k = 6.0$ results as tables of the scattering amplitude $|T|$ at scattering angles 0° and 180° as a function of N and NPW in Tables I–IV. For the TMM results we also show the number of mesh points NGP used in the Gaussian quadrature procedure for evaluating the matrix elements $H_{lm,l'm}$ and $J_{lm,l'm}$.

Finally, we display on these tables the condition numbers C No. of the matrices to be inverted, $1 - H$ for the TMM and $1 - 2K$ for the HIEM. The condition number of a matrix A was defined by Turing[12] to be

$$C \text{ No.} = n^{-1} N(A)^{1/2} N(A^{-1})^{1/2}, \tag{19a}$$

where n is the dimension of A and

$$N(A) = \sum_{i=1}^{n} \sum_{j=1}^{n} |A_{ij}|^2 \tag{19b}$$

is the norm of A. It serves as a measure of how much small changes in A are amplifed in the calculation of A^{-1}. Thus it serves to indicate how seriously the value of the scattering amplitude $|T|$ is affected by the small numerical inaccuracies present in H or K. The condition number provides a measure of the calculational stability.

An ideally well-conditioned matrix has C No. = 1

TABLE II. Same as Table I except that $a = 0.5$.

			$a = 0.5$ $k = 6.0$					
	HIEM					TMM		
N	C No.	$\lvert T(0°)\rvert$	$\lvert T(180°)\rvert$	NGP	NPW	C No.	$\lvert T(0°)\rvert$	$\lvert T(180°)\rvert$
10	2.97	1.674	0.5991	48	3	1.05	0.5322	0.4815
24	1.31	1.086	0.9565	48	4	1.11	0.7297	0.3961
46	1.21	1.166	0.3570	48	6	2.26	0.9845	0.7304
78	1.13	1.128	0.4651	48	8	8.2×10^3	0.9800	0.4678
114	1.09	1.120	0.4624	56	8	5.6×10^3	1.065	0.5567
156	1.07	1.116	0.4625	64	8	1.8×10^4	1.165	0.4368
				48	9	6.3×10^6	0.9979	0.4828
				48	10	overflow		

TABLE III. Same as Table I except that $a = 0.2$.

	HIEM			$a = 0.2$ $k = 6.0$		TMM		
N	C No.	$\|T(0°)\|$	$\|T(180°)\|$	NGP	NPW	C No.	$\|T(0°)\|$	$\|T(180°)\|$
8	1.82	0.3940	0.3318	104	3	1.67	0.1800	0.2854
16	1.55	0.3525	0.5745	104	4	3.92	0.2329	0.3614
26	1.31	0.3660	0.5350	72	4	3.92	0.2329	0.3614
40	1.19	0.3699	0.4757	64	4	3.92	0.2329	0.3614
60	1.13	0.3711	0.5006	104	5	17.5	0.2478	0.3800
82	1.09	0.3705	0.5028	104	6	117	0.3731	0.1441
106	1.07	0.3707	0.5043	104	7	994	0.5373	0.3739
134	1.06	0.3706	0.5047	104	8	1.0×10^4	0.3830	0.5394
				88	8	1.0×10^4	0.8631	0.5119
				120	8	1.0×10^4	1.048	0.7245
				80	9	1.8×10^5	overflow	

whereas an ill-conditioned matrix has C No. $\gg 1$. From the tables we see that the condition number of $1 - 2K$ of the HIEM becomes smaller with increasing N and very quickly assumes a value close to one. On the other hand, the condition number of $1 - H$ of the TMM grows rapidly greater with increasing NPW and very quickly attains values several orders of magnitude greater than one. The condition number is relatively independent of the aspect ratio c/a for $1 - 2K$ but for $1 - H$ its growth with NPW is amplified by increasing c/a.

Examination of the values of $|T|$ displayed on Tables I–IV reveals that they tend to converge quite smoothly with increasing N for all values of the aspect ratio for the HIEM. The convergence rate of the TMM is better than that of the HIEM for the spherical case, but it is worse than that of the HIEM for the three nonspherical cases, becoming rapidly worse as the aspect ratio is increased.

The stability of the TMM calculation can be gauged by how sensitive the result for $|T|$ is to changes in NGP, the number of mesh points used in the gaussian quadrature procedure for evaluating the elements of the matrices J and H. Results for such variations of NGP are shown on each of the four tables. There is no sensitivity seen in the spherical case, but the sensitivity increases noticeably with increasing aspect ratio.

Curiously enough, the stability does not always seem to be correlated with the C No. Thus comparison of the NPW = 8 results on Tables I and II shows that the $a = 1.0$ results are stable while the $a = 0.5$ results are somewhat unstable although the C No. values are about the same in the two cases. On the other hand, the comparison of the NPW = 4 results with the NPW = 8 results, both on Table III, reveals that the NPW = 4 results have C No. = 4 and are stable while the NPW = 8 results have C No. = 10^4 and are unstable.

III. DISCUSSION

The numerical difficulties of the TMM are well known. Methods for dealing with these difficulties have been suggested by several people.[13–20] The purpose of our calculations was to get some measure of the significance of the freedom from such numerical difficulties of the HIEM by programming the TMM and HIEM in a similar way and by using those programs on the same computer to analyze the same problems.

One method for overcoming the poor convergence of the TMM found here would be to base it on an expansion in terms of a set of spheroidal waves instead of spherical waves.[21] This would be ideally efficient for the calculation of scattering by spheroidal targets. It would be more efficient than the HIEM just as our calculations show the TMM using a spherical basis is superior to the HIEM for scattering by spheres. However, we can expect that the convergence of the spheroidal basis TMM would deteriorate to the extent that the shape of the target departs from that of a spheroid

TABLE IV. Same as Table I except that $a = 0.1$.

	HIEM			$a = 0.1$ $k = 6.0$		TMM		
N	C No.	$\|T(0°)\|$	$\|T(180°)\|$	NGP	NPW	C No.	$\|T(0°)\|$	$\|T(180°)\|$
18	2.60	0.1448	0.2487	96	2	1.60	0.0306	0.0993
24	2.01	0.1382	0.2670	96	3	4.83	0.0269	0.1356
34	1.62	0.1284	0.2785	96	4	29.2	0.0474	0.1780
44	1.43	0.1315	0.2930	96	5	299	0.0411	0.1933
60	1.28	0.1365	0.3018	96	6	4.2×10^3	0.2749	0.1164
74	1.21	0.1368	0.3003	96	7	6.7×10^4	0.5212	0.1928
92	1.61	0.1355	0.2986	88	7	6.5×10^4	1.481	1.099
114	1.13	0.1344	0.2967	104	7	6.9×10^4	0.9770	0.5898
132	1.11	0.1348	0.2974	88	8	1.7×10^5	overflow	

whereas the convergence of the HIEM would be affected very little.

There is one problem that the HIEM encounters at higher frequencies than we have employed in the calculations done here. That is the problem of characteristic frequencies. When the scattering is characterized by homogeneous boundary conditions on the surface of a scatterer, as it is for rigid body scattering, then the solution of the Helmholtz integral equation becomes nonunique at those frequencies at which standing waves consistent with the homogeneous boundary conditions could exist in the volume occupied by the scatterer. At those frequencies the Helmholtz integral equation becomes numerically unstable.

There are several methods[5] that have been shown to be effective in overcoming that numerical instability. In a recently published test[7] of the HIEM we verified that the method of H. A. Schenck,[5] called the combined Helmholtz integral equation formulation (CHIEF) is easily employed for the purpose. In the CHIEF the HIEM is supplemented by a few null-field equations, Fredholm integral equations of the first kind derived from the same Helmholtz formula used to derive the HIEM, and these serve to eliminate the numerical instability.

The superiority of the HIEM over the TMM for numerical calculations of the scattering of waves by nonspherical targets is certainly very striking. We expect that the future will see extensive application of the HIEM to a wide variety of scattering problems.

ACKNOWLEDGMENTS

The author is grateful to L. L. Foldy for many helpful discussions of the subject matter of this paper. He is also grateful to Case Western Reserve University for the use of its computing facilities.

[1]P. C. Waterman, Proc. IEEE **53**, 805 (1965).
[2]P. C. Waterman, J. Acoust. Soc. Am. **45**, 1417 (1968).
[3]B. Peterson and S. Strom, J. Acoust. Soc. Am. **57**, 2 (1975); P. C. Waterman, J. Acoust. Soc. Am. **60**, 567 (1976); A. Bostrom, J. Acoust. Soc. Am. **67**, 390 (1980).
[4]Y.-H. Pao and V. Varatharajulu, J. Acoust. Soc. Am. **59**, 1361 (1976); V. Varatharajulu and Y.-H. Pao, J. Acoust. Soc. Am. **60**, 566 (1976).
[5]G. Chertock, J. Acoust. Soc. Am. **36**, 1305 (1964); L. G. Copely, J. Acoust. Soc. Am. **41**, 807 (1966); H. A. Schenck, J. Acoust. Soc. Am. **44**, 41 (1967); A. J. Burton and G. F. Miller, Proc. R. Soc. London Ser. A **323**, 201 (1971); W. L. Meyer, W. A. Bell, M. P. Stallybrass, and B. T. Zinn, J. Acoust. Soc. Am. **65**, 631 (1979); C. M. Piaszeczyk and J. M. Klosner, "Acoustic Radiation from Vibrating Surfaces at Characteristic Frequencies," Polytechnic Institute of New York, Rep. M/AE 82–11.
[6]G. B. Brundrit, J. Mech. Appl. Math. XVIII, 473 (1965).
[7]W. Tobocman, "Calculation of Acoustic Wave Scattering by Means of the Helmholtz Integral Equation.I," J. Acoust. Soc. Am. **76**, 599 (1984).
[8]W. Tobocman, "Calculation of Acoustic Wave Scattering by Means of the Helmholtz Integral Equation.II," C. W. R. U. Rep. (1984).
[9]B. B. Baker and E. T. Copson, *Mathematical Theory of Huygens' Principle* (Oxford U. P., London, 1950).
[10]V. K. Varadan, V. J. Varadan, L. R. Dragonette, and L. Flax, J. Acoust. Soc. Am. **71**, 22 (1982).
[11]R. D. Spence and S. Grange, J. Acoust. Soc. Am. **23**, 701 (1951).
[12]A. M. Turing, Q. J. Mech. Appl. Math. **1**, 287 (1948).
[13]P. C. Waterman, Phys. Rev. D **3**, 825 (1971); R. H. T. Bates and D. J. N. Wall, Philos. Trans. R. Soc. London Ser. A **287**, 45 (1977).
[14]D. J. N. Wall, J. Phys. A: Math. Gen. **11**, 749 (1978).
[15]D. J. N. Wall, "Methods of Overcoming Numerical Instabilities Associated with the *T*-matrix Method," in *Acoustic, Electromagnetic, and Elastic Wave Scattering*, edited by V. V. Varadan and V. K. Varadan (Pergamon, New York, 1980).
[16]W. M. Visscher, J. Appl. Phys. **51**, 825 (1980).
[17]P. C. Waterman, "Survey of the *T*-matrix Method," in *Acoustic, Electromagnetic, and Elastic Wave Scattering*, edited by V. V. Varadan and V. K. Varadan (Pergamon, New York, 1980.
[18]G. Kirstensson and P. C. Waterman, J. Acoust. Soc. Am. **72**, 612 (1982).
[19]M. F. Werby and L. H. Green, J. Acoust. Soc. Am. **74**, 625 (1983).
[20]M. F. Werby, "A Coupled Higher-order *T*-matrix," NORDA Rep. (1984).
[21]R. H. Hackman, J. Acoust. Soc. Am. **75**, 35 (1984); J. Acoust. Soc. Am. Suppl. 1 **75**, S53 (1984).